

Free-standing and highly conductive PEDOT nanowire films for high-performance all-solid-state supercapacitors

Dan Ni^a, Yuanxun Chen^a, Haijun Song^a, Congcong Liu^a, Xiaowei Yang^a, Kefeng
Cai^{a,b,*}

^a Key Laboratory of Advanced Civil Engineering Materials (Tongji University), Ministry of
Education, School of Materials Science & Engineering, Tongji University, 4800 Caoan Road,
Shanghai 201804, China

^b Shanghai Key Laboratory of Development and Application for Metal-Functional Materials

*Corresponding author: kfcai@tongji.edu.cn

Figure captions

Figure S1. (a) TEM image of the PEDOT NWs. (b) The size distribution of the PEDOT NWs in (a) measured by Nano Measurer. (c) The electrical conductivity of the flexible PEDOT film as a function of bending times.

Figure S2. The XPS S2p core-level spectra of (a) the 80-PEDOT and (b) the NM-80-PEDOT.

Figure S3. (a) XRD patterns and (b) Raman spectra of the NM-PEDOT and M-PEDOT NW films.

Figure S4. CV curves at different scan rates and GCD curves at different current densities for the 60-PEDOT (a, b), 80-PEDOT (c, d), 120-PEDOT (e, f) and 140-PEDOT (g, h), respectively.

Figure S5. The areal specific capacitance as a function of active mass in 1 M H₂SO₄ at 0.5 mA/cm².

Figure S6. CV curves at different scan rates and GCD curves at different current densities for the NM-80-PEDOT.

Figure S7. (a) CV curves at 100 mV/s, (b) GCD curves at 0.5 mA/cm² and (c) the specific capacitance as a function of current densities for the NM-80-PEDOT and 80-PEDOT in a 1 M H₂SO₄ electrolyte, respectively. (d) The electrical conductivity of

the NM-80-PEDOT and 80-PEDOT.

Figure S8. (a) FTIR spectra of the PD0.08 and 0.08 M dopamine dissolved in 1 M H_2SO_4 , and (b) the enlarged plot of (a) from 1500 to 3000 cm^{-1} .

Figure S9. CV curves at different scan rates and GCD curves at different current densities for the 60-PEDOT in PD0.05 (a, b), PD0.08 (c, d) and PD0.10 (e, f), respectively.

Equation 1. The redox reaction of phenolic hydroxyl group/quinoid carbonyl group in polydopamine.

Figure S10. (a) Electrical conductivity of the PEDOT film as a function of H_2SO_4 concentration, and (b) UV-Vis-NIR spectra of the pristine and the 1 M H_2SO_4 treated PEDOT NW films.

Figure S11. The voltage decay curves of the 140-PEDOT electrode in (a) 1 M H_2SO_4 electrolyte and (b) PD 0.08 electrolyte.

Preparation of PEDOT NWs by the method reported in refs.[1, 2]

The typical synthetic procedure is as follows: 30 mmol SDS was dissolved in 100 mL deionized (DI) water followed by addition of an aqueous solution of FeCl₃ with stirring at 50 °C. 750 μL EDOT monomer was slowly introduced into the solution with continuous stirring, and the polymerization reaction proceeded for 6 h at 50 °C and then the solution was taken out of the oil bath and cooled to room temperature. Finally, the black product was washed with DI water and methanol for several times.

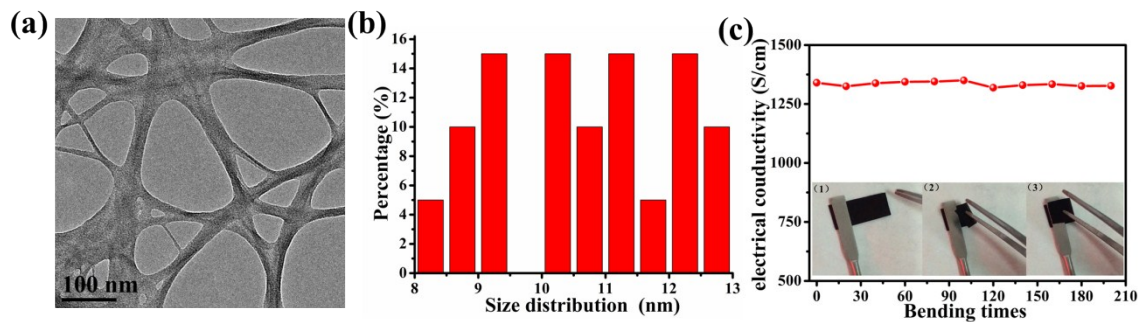


Figure S1. (a) A typical TEM image of the PEDOT NWs, (b) the size distribution of the PEDOT NWs in (a) measured by Nano Measurer, (c) the electrical conductivity of the flexible PEDOT film as a function of bending times.

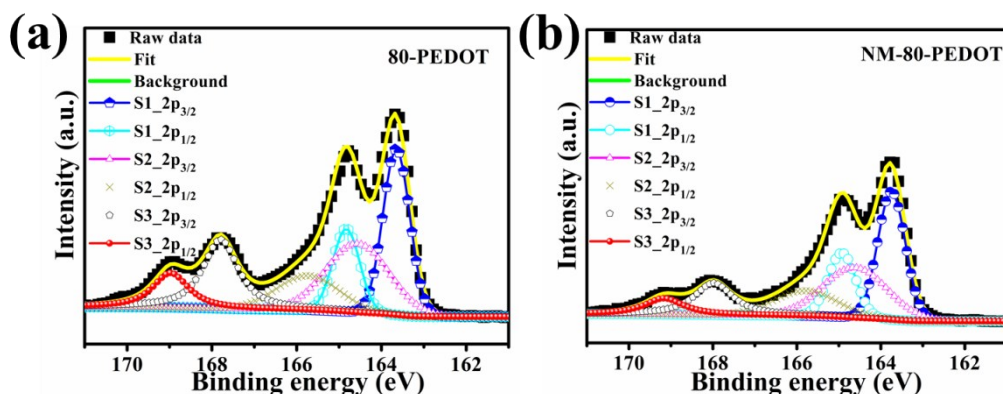


Figure S2. The XPS S2p core-level spectra of (a) the 80-PEDOT and (b) the NM-80-PEDOT.

Figure S2 describes the XPS S2p core-level spectra of the 80-PEDOT and NM-80-PEDOT, respectively. As shown in Figure S2, the S2p signals include three components, and each one can be fitted with a spin-split doublet, S2p_{1/2} and S2p_{3/2}, with the energy splitting of 1.2 eV, an area ratio of 1:2 and the same full width half maximum [2]. For the sulfur atom from PEDOT chains, two doublets respectively at 163.6 eV (S1_2p_{3/2}) and 164.8 eV (S1_2p_{1/2}), and 164.6 eV (S2_2p_{3/2}) and 165.8 eV (S2_2p_{1/2}) are corresponding to the neutral (S⁰) and partially oxidized state (S^{δ+}) in the polymer chains [3]. The last component located at 167.8 eV (S3_2p_{3/2}) and 169.0 eV (S3_2p_{1/2}) are ascribed to the sulfur atom of the dodecyl sulfate anions (DS⁻) [4], indicating the incorporation of DS⁻ anions in the films. The doping levels of the samples can be estimated from their corresponding S2p signals. The doping level is calculated using the equation: $Doping\ level = A_{S_{DS^-}} / (A_{S^0} + A_{S^{\delta+}})$, where A_{S⁰}, A_{S^{δ+}}, and A_{S_{DS⁻}} stand for the peak area of the neutral PEDOT, oxidized PEDOT, sulfur atom from DS⁻, respectively. The doping level is calculated to be 39.0% and 28.4% for the 80-PEDOT and NM-80-PEDOT samples, respectively.

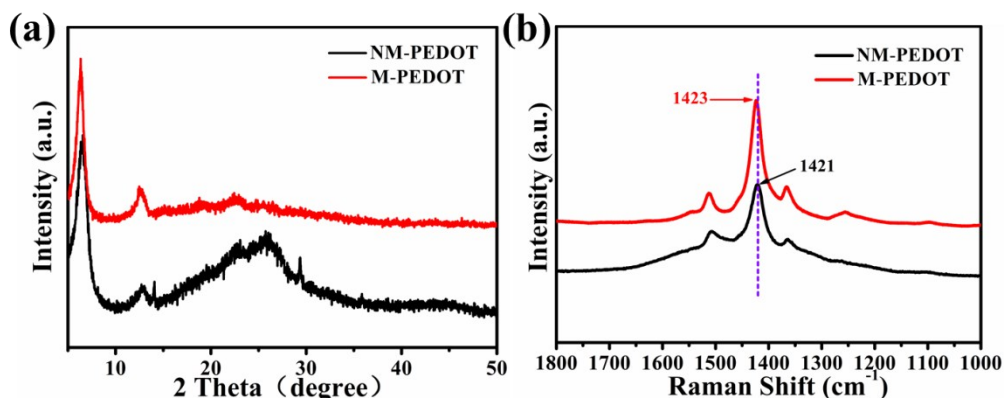


Figure S3. (a) XRD patterns and (b) Raman spectra of the NM-PEDOT and M-PEDOT NW films.

XRD patterns of the NM-PEDOT (prepared by the not modified method) and M-PEDOT (prepared by our modified method) NW films are shown in Figure S3a. Obviously, both the films exhibit two distinct peaks: one very strong at $2\theta=6.4^\circ$ and the other weaker at $2\theta=12.8^\circ$. The sharp and strong peak at $2\theta=6.4^\circ$ corresponds to the interchain packing along an orthorhombic a-axis [1] and is the typical characteristic peak of PEDOT NWs. The peak at $2\theta=12.8^\circ$ is the (200) plane reflections of the (100) plane ($2\theta=6.4^\circ$). The peaks of the M-PEDOT are sharper, which means a more ordered structure of the M-PEDOT film [1]. In addition, there is a strong and broad peak centered at $2\theta=25.6^\circ$ for the NM-PEDOT NW film, which is a characteristic of the disordered structure of PEDOT macromolecular chains [4]. The higher degree of ordering of the chain packing leads to higher electrical conductivity [5].

Raman spectroscopy is an effective characterization method to study the doping behavior of conducting polymers. Figure S3b shows Raman spectra of the NM-

PEDOT and M-PEDOT NW films. Raman band between 1400 and 1500 cm^{-1} originating from $\text{C}\alpha=\text{C}\beta$ stretching vibration of PEDOT [6] shifts to a higher wavenumber for the M-PEDOT NW film, suggesting the increasing doping level of the film, and hence the higher electrical conductivity of the film [7, 8].

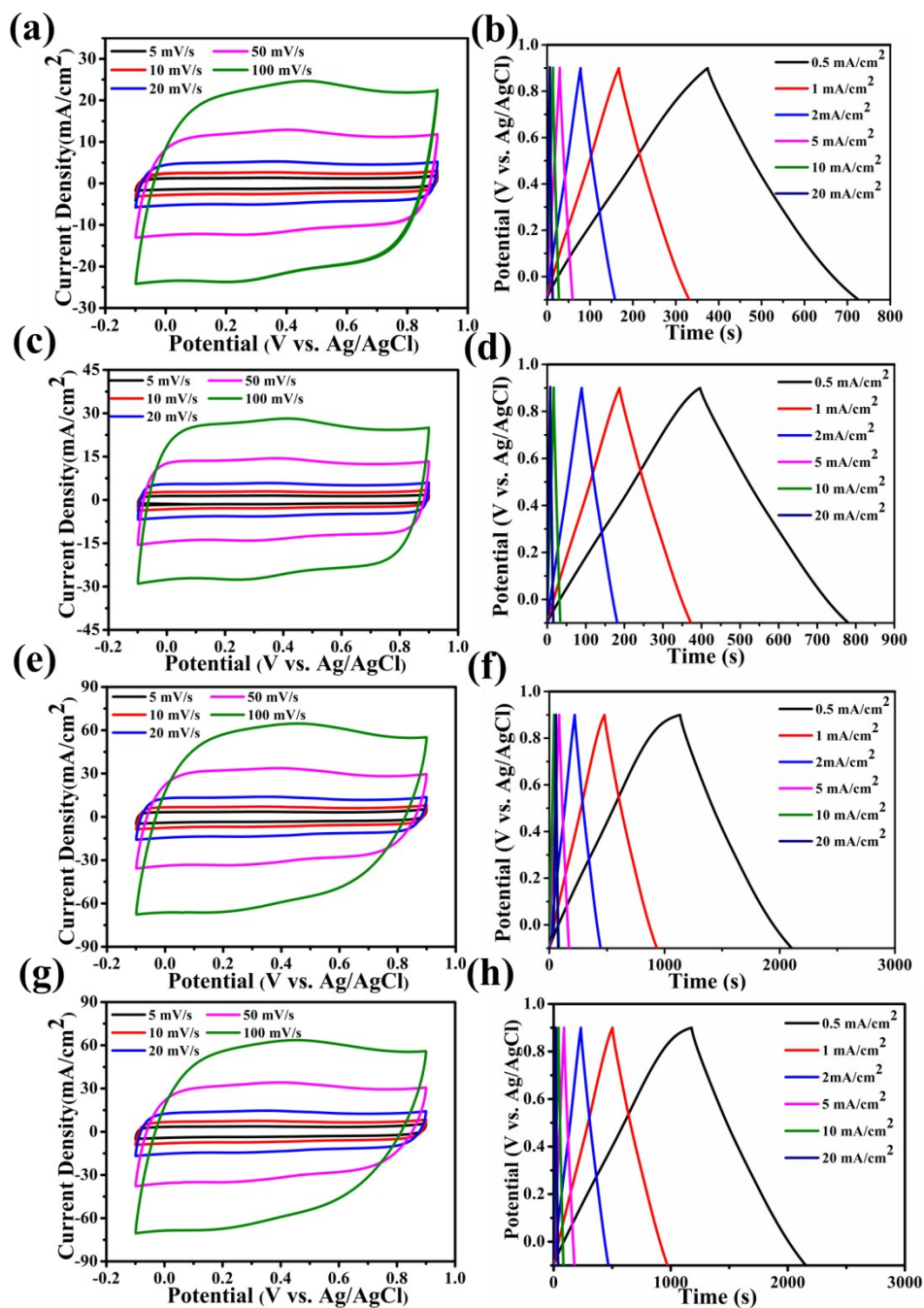


Figure S4. CV curves at different scan rates and GCD curves at different current densities for the 60-PEDOT (a, b), 80-PEDOT (c, d), 120-PEDOT (e, f) and 140-PEDOT (g, h), respectively.

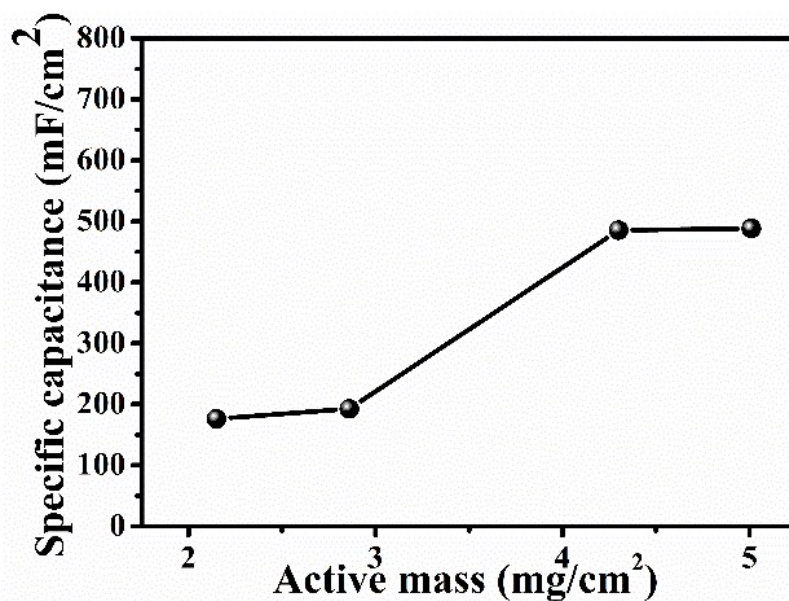


Figure S5. The areal specific capacitance as a function of active mass in 1 M H₂SO₄ at 0.5 mA/cm².

Figure S5 illustrates the areal specific capacitance as a function of active mass in 1 M H₂SO₄ at 0.5 mA/cm². As is shown, the specific capacitance increases with the increasing active mass: it increases from 176.0 mF/cm² to 488.2 mF/cm² when the active mass loading increases from 2.15 to 5.01 mg/cm², indicating good material utilization [9].

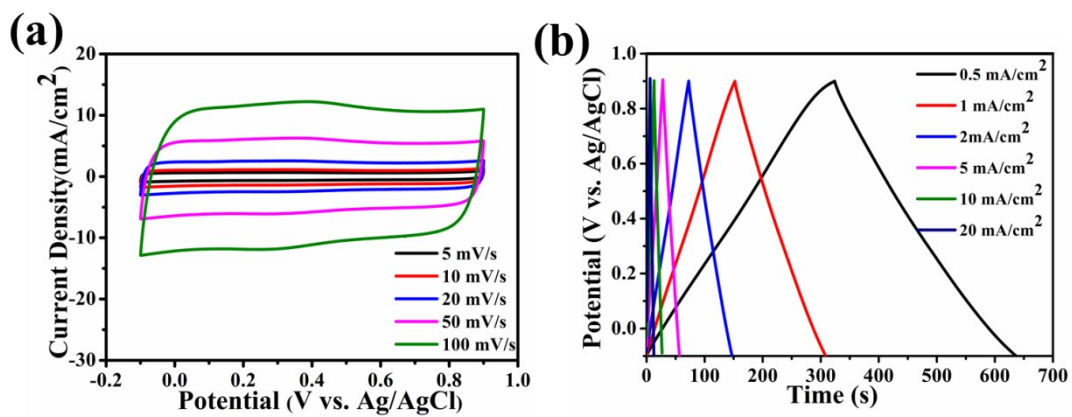


Figure S6. CV curves at different scan rates (a) and (b) GCD curves at different current densities for the NM-80-PEDOT.

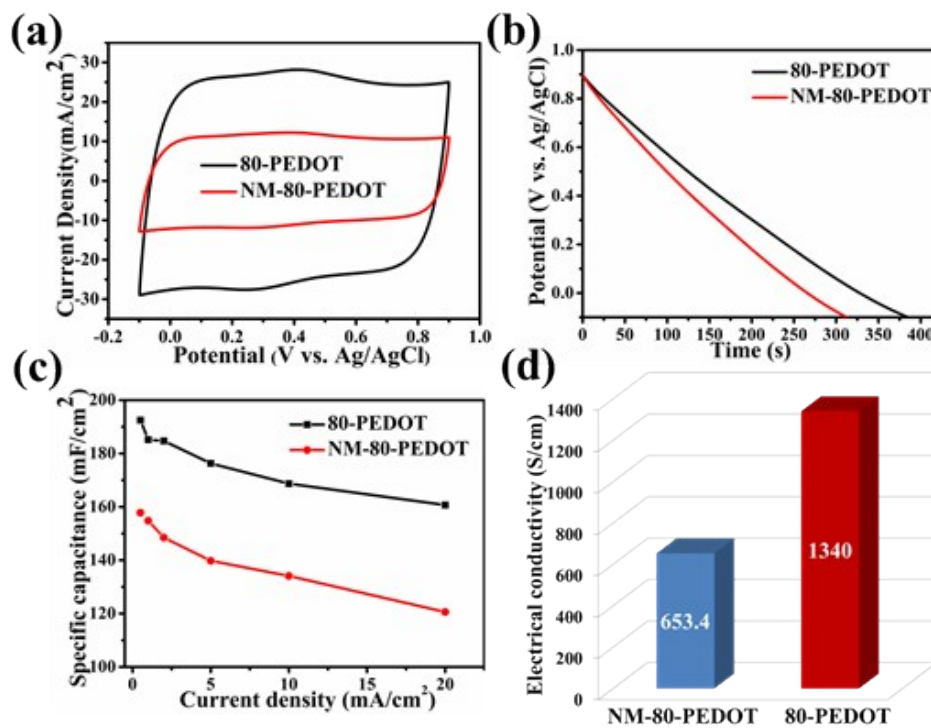


Figure S7. (a) CV curves at 100 mV/s, (b) GCD curves at 0.5 mA/cm² and (c) the specific capacitance as a function of current densities for the NM-80-PEDOT and 80-PEDOT in a 1 M H₂SO₄ electrolyte, (d) The electrical conductivity of the NM-80-PEDOT and 80-PEDOT.

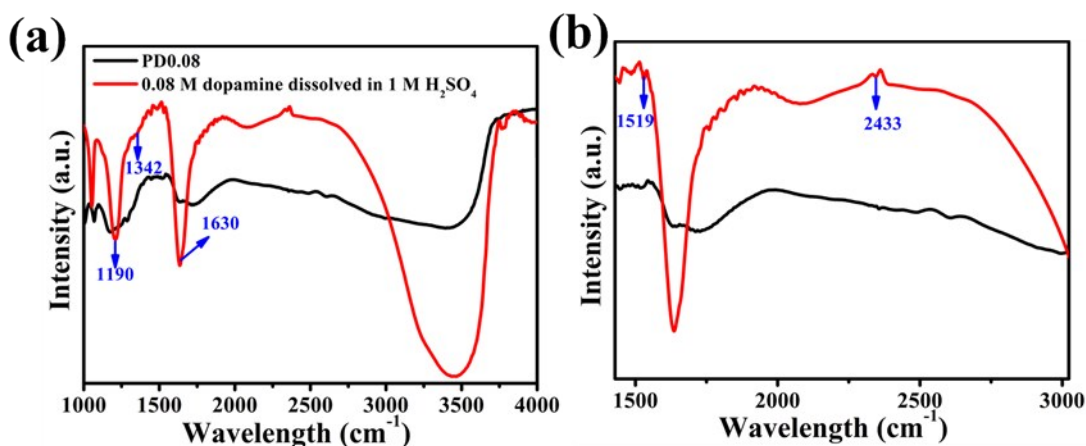


Figure S8. (a) FTIR spectra of the PD0.08 and 0.08 M dopamine dissolved in 1 M H₂SO₄, and (b) an enlarged plot of (a) from 1500 to 3000 cm⁻¹.

After cycling for 36 h, the transparent dopamine solutions were transformed into claybank solutions, and its composition was investigated by FTIR spectroscopy. The FTIR spectra of the PD0.08 and the dopamine solution before cycling are shown in Figure S8a-b. In Figure S8a, dopamine shows relatively broad and strong bands in the region of 3000-3600 cm⁻¹, which are assigned to the intermolecular hydrogen bonds existing in dopamine molecules. The peak at 1190 cm⁻¹ is due to the C-O symmetry vibration; the peak at 2433 cm⁻¹ is assigned to the N-H stretching vibration; the peak at 1519 cm⁻¹ is due to the NH₂ scissoring vibration modes. Besides, the band corresponding to C=C stretching vibration of indole is also observed at 1630 cm⁻¹. For the PD0.08, the peaks at 1190, 1342 (CH₂ bending vibration), 1519 (NH₂ scissoring vibration), 2433 and 1630 cm⁻¹ weaken or disappear, indicating that intramolecular cyclization reaction occurs of the dopamine and forms the indole derivatives (polydopamine) [10, 11].

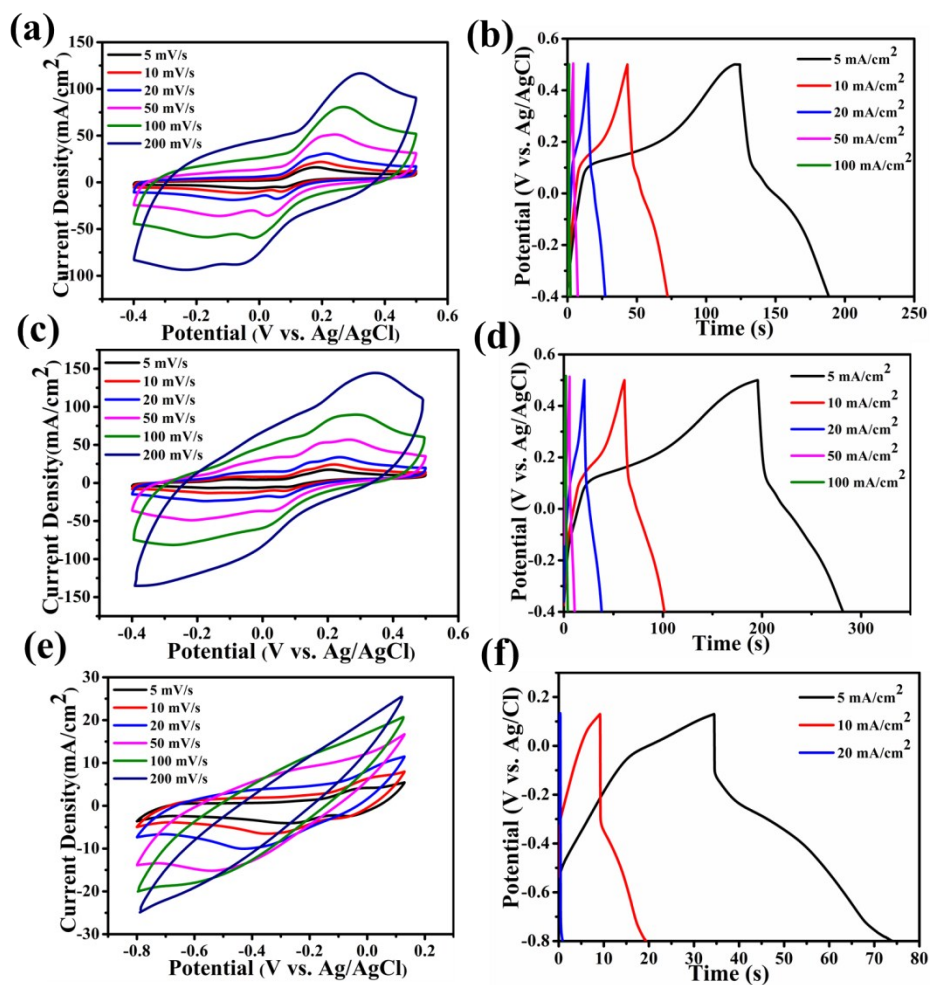
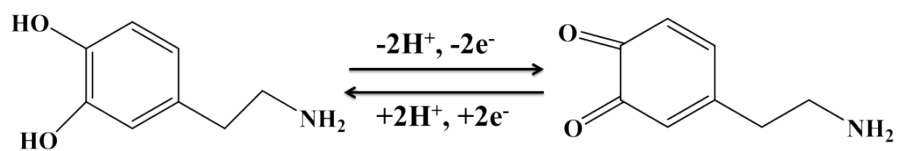


Figure S9. CV curves at different scan rates and GCD curves at different current densities for the 60-PEDOT in PD0.05 (a, b), PD0.08 (c, d) and PD0.10 (e, f), respectively.



Equation 1. The redox reaction of phenolic hydroxyl group/quinoid carbonyl group in polydopamine

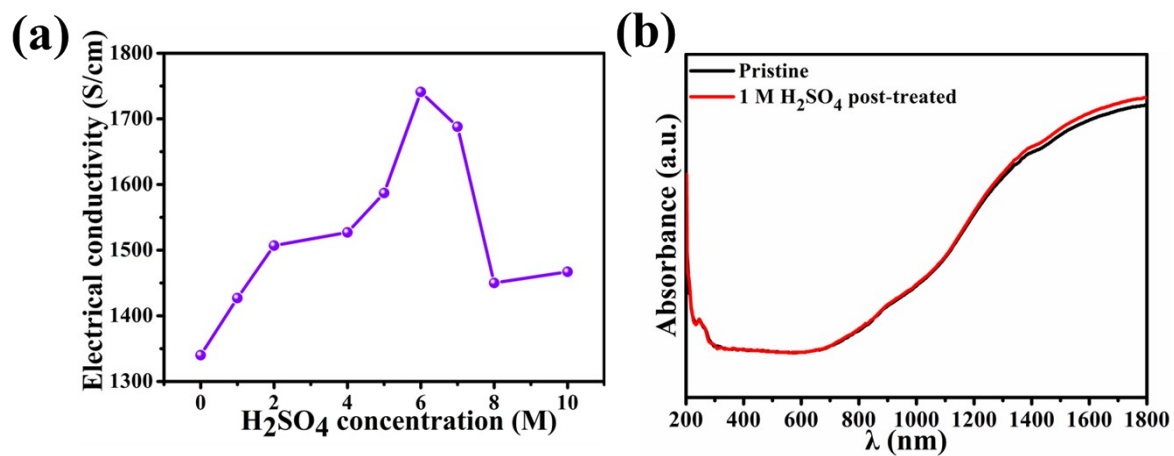


Figure S10. (a) Electrical conductivity of the PEDOT film as a function of H_2SO_4 concentration for treatment, and (b) UV-Vis-NIR spectra of the pristine and the 1 M H_2SO_4 treated PEDOT NW films.

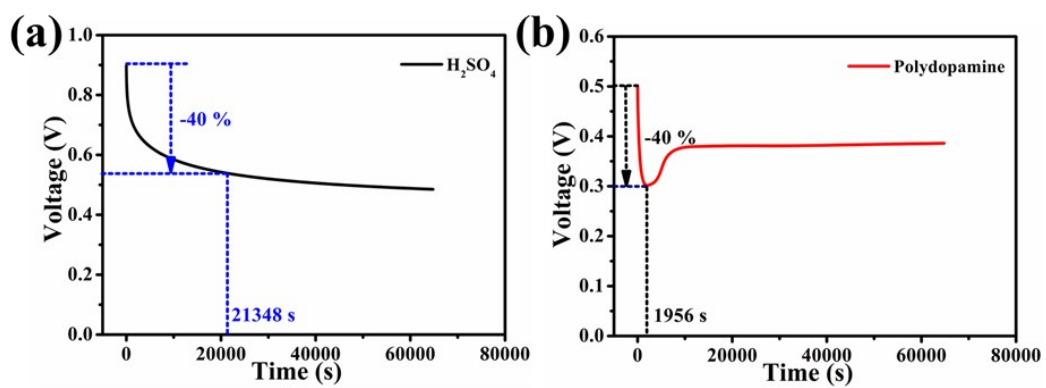


Figure S11. The voltage decay curves of the 140-PEDOT electrode in (a) 1 M H₂SO₄ electrolyte and (b) PD 0.08 electrolyte.

References:

- [1] M.G. Han, S.H. Foulger, Facile synthesis of poly(3,4-ethylenedioxythiophene) nanofibers from an aqueous surfactant solution, *Small*, 2 (2006) 1164-1169.
- [2] J. Zhang, K. Zhang, F. Xu, S. Wang, Y. Qiu, Thermoelectric transport in ultrathin poly(3,4-ethylenedioxythiophene) nanowire assembly, *Composites Part B Engineering*, 136 (2017) 234-240.
- [3] J.L. Duvail, P. Rétho, V. Fernandez, G. Louarn, A. P. Molinié, O. Chauvet, Effects of the Confined Synthesis on Conjugated Polymer Transport Properties, *J.Phys.Chem.B*, 108 (2004) 18552-18556.
- [4] J. Zhao, D. Tan, G. Chen, A strategy to improve the thermoelectric performance of conducting polymer nanostructures, *Journal of Materials Chemistry C*, (2016) 47-53.
- [5] X. Hu, G. Chen, X. Wang, H. Wang, Tuning thermoelectric performance by nanostructure evolution of a conducting polymer, *Journal of Materials Chemistry A*, 3 (2015) 20896-20902.
- [6] J. Ouyang, Q. Xu, C.W. Chu, Y. Yang, G. Li, J. Shinar, On the mechanism of conductivity enhancement in poly(3,4-ethylenedioxythiophene):poly(styrene sulfonate) film through solvent treatment, *Polymer*, 45 (2004) 8443-8450.
- [7] W.W. Chiu, J. Travas-Sejdic, R.P. Cooney, G.A. Bowmaker, Studies of dopant effects in poly(3,4-ethylenedioxythiophene) using Raman spectroscopy, *Journal of Raman Spectroscopy*, 37 (2010) 1354-1361.
- [8] M. Reyesreyes, I. Cruzcruz, R. Lópezsandoval, Enhancement of the Electrical Conductivity in PEDOT:PSS Films by the Addition of Dimethyl Sulfate, *Journal of*

Physical Chemistry C, 114 (2010) 20220-20224.

[9] K. Shi, X. Yang, E.D. Cranston, I. Zhitomirsky, Efficient Lightweight Supercapacitor with Compression Stability, *Advanced Functional Materials*, 26 (2016) 6437-6445.

[10] T. Xiong, W.S.V. Lee, L. Chen, T.L. Tan, X. Huang, J. Xue, Indole-based conjugated macromolecules as a redox-mediated electrolyte for an ultrahigh power supercapacitor, *Energy & Environmental Science*, 10 (2017) 2441-2449.

[11] F. Yu, S. Chen, Y. Chen, H. Li, L. Yang, Y. Chen, Y. Yin, Experimental and theoretical analysis of polymerization reaction process on the polydopamine membranes and its corrosion protection properties for 304 Stainless Steel, *Journal of Molecular Structure*, 982 (2010) 152-161.